ISSN 1674-1056
http://cpb.iphy.ac.cn
http://iopscience.iop.org/cpb
中国物理 B
Chinese Physics
中国物理 Chinese Physics B

Single-doped charged gold cluster with highly selective catalytic activity for the reduction of SO_2 by CO: First-principles study

Yan-Ling Hu(胡燕玲), Hao-Ran Zhu(祝浩然), Shi-Hao Wei(韦世豪)
Citation: Chin. Phys. B . 2019, 28(11): 113101 . **doi:** 10.1088/1674-1056/ab4cdd
Journal homepage: http://cpb.iphy.ac.cn; http://iopscience.iop.org/cpb

What follows is a list of articles you may be interested in

Effect of nickel segregation on CuΣ9 grain boundary undergone shear deformations

Xiang-Yue Liu(刘湘月), Hong Zhang(张红), Xin-Lu Cheng(程新路)
Chin. Phys. B . 2018, 27(6): 063103 . **doi:** 10.1088/1674-1056/27/6/063103

Spin polarization and dispersion effects in emergence of roaming transition state for nitrobenzene isomerization

Zhi-Yuan Zhang(张志远), Wan-Run Jiang(姜万润), Bo Wang(王波), Yan-Qiang Yang(杨延强), Zhi-Gang Wang(王志刚)
Chin. Phys. B . 2018, 27(1): 013102 . **doi:** 10.1088/1674-1056/27/1/013102

Lattice stability and the effect of Co and Re on the ideal strength of Ni: First-principles study of uniaxial tensile deformation

Minru Wen(文敏儒), Chong-Yu Wang(王崇愚)
Chin. Phys. B . 2017, 26(9): 093106 . **doi:** 10.1088/1674-1056/26/9/093106

First-principles study of solute diffusion in Ni_3Al

Shaohua Liu(刘少华), Zi Li(李孜), Chongyu Wang(王崇愚)
Chin. Phys. B . 2017, 26(9): 093102 . **doi:** 10.1088/1674-1056/26/9/093102

First-principles study of the electronic and optical properties of the (Y, N)-codoped anatase TiO_2photocatalyst

Lin Yan-Ming,Jiang Zhen-Yi,Hu Xiao-Yun,Zhang Xiao-Dong,Fan Jun,Miao Hui,Shang Yi-Bo
Chin. Phys. B . 2012, 21(3): 033103 . **doi:** 10.1088/1674-1056/21/3/033103

Single-doped charged gold cluster with highly selective catalytic activity for the reduction of SO_2 by CO: First-principles study*

Yan-Ling Hu(胡燕玲), Hao-Ran Zhu(祝浩然), and Shi-Hao Wei(韦世豪)†

Department of Microelectronic Science and Engineering, School of Physical Science and Technology, Ningbo University, Ningbo 315211, *China*

(Received 17 September 2019; revised manuscript received 3 October 2019; published online 25 October 2019)

It is important for environmental protection to search for catalysts with excellent performance and cost-effective to reduce SO_2 by CO. In this work, using first-principles calculation, we have studied the catalytic performance of Au_5M^n (M = Ni, Pd, Pt, Cu, Ag, Au; $n = 1, 0, -1$) clusters, and showed that, by giving a negative charge to the Au_5M (M = Cu, Ag, Au, Pd) clusters, we could improve the selectivity of SO_2 and avoid effectively catalyst CO poisoning simultaneously. At the same time, the catalytic reaction rate for the reduction of SO_2 by CO with Au_5M^- (M = Cu, Ag, Au, Pd) clusters is greatly improved when the Au_5M clusters are charged. These advantages can be well explained by the charge transfer between the clusters and adsorbed molecules, which means that we can effectively control the performance of the catalyst. The equilibrium structures of Au_5M^n (M = Ni, Pd, Pt, Cu, Ag, Au; $n = 1, 0, -1$) clusters without or with adsorbed SO_2 or CO molecule are also discussed, and the most stable geometrical structures of Au_5M^n-ML (ML = SO_2, CO, SO, and COS) can be explained very well by the match of orbitals symmetry and density of electron cloud through their frontier molecular orbitals. Considering the catalyst cost (Cu is much cheaper than Ag and Au), selectivity of SO_2, and effectively avoiding the catalyst CO poisoning, we propose that Au_5Cu^- is an ideal catalyst for getting rid of SO_2 and CO simultaneously.

Keywords: bimetallic clusters, catalyst, first-principles, electronic structure

PACS: 31.15.Ar, 36.40.Cg, 73.22.–f **DOI:** 10.1088/1674-1056/ab4cdd

1. Introduction

Sulfur dioxide (SO_2) gains wide attention for perniciousness to environment and human health.[1–4] Every year, the combustion of fossil fuels leads to the high level of SO_2 emission to the atmosphere from both stationary and mobile sources. Thus the capture and reduction of SO_2 content are important in the environment protection. In recent years, much research efforts have been focused on the reduction of SO_2 to elemental sulfur, which would provide an effective solution for the above mentioned problems and ease the shortage of elemental sulfur. SO_2 can be reduced by various reducing agents such as hydrogen (H_2),[5,6] carbon monoxide (CO),[6–8] methane (CH_4),[8,9] and carbon (C).[10,11] Compared with other gas, the reduction reaction of SO_2 and CO should have a higher SO_2 conversion rate at relatively lower temperature through appropriate catalyst, and CO always coexists with SO_2 in petrochemical waste gas.[12] The main reaction associated with this process is described as follows:

$$SO_2 + 2CO \longrightarrow S + 2CO_2.$$

A variety of catalysts, such as alumina supported transition metals,[12] Pt–Au bimetallic catalyst,[13] and La_2O_2S catalyst,[14] were developed for the selective reduction of SO_2. These catalysts show a good catalytic performance for the SO_2 reduction using CO as an reducing reagent, but the alumina supported transition metals typically need to be activated by reducing gases at high temperature,[15] and the use of noble metal Pt and rare earth element La is limited on account of their prices and amounts. In addition, when using CO to reduce SO_2, the noble metal catalyst like Pt will suffer from the CO adsorption poisoning,[16] thereby there is an urgent need to pursue the catalysts outside of it with catalytic performance and selectivity for SO_2 reduction, which is still a significant challenge.

Bulk metallic gold typically exhibits a quite low chemical and catalytic activity for a long time, owing to its deep-lying valence d band and very decentralized valence s, p orbits.[17] About more than three decades ago, this rule was broken by Haruta' group, they discovered that small Au nanoparticles (NPs) supported on the 3d metallic oxide could catalyze CO oxidation below room temperature.[18] There after, a large amount of experimental and theoretical researches have suggested that the catalytic activity of the Au particles depends on their size and shape, also including the property of interaction with the supported surface.[18–28]

So far, gold-based materials can serve as high-efficiency catalysts for accelerating a lot of reactions, such as CO oxidation,[18–21,23,24,29,30] O_2 dissociation,[31,32] water-gas shift reaction,[21,33,34] selective oxidation of alcohols,[35–37] etc. However, the pure Au catalysts are relative unstable,

*Project supported by the National Natural Science Foundation of China (Grant No. 11375091), the Natural Science Foundation of Zhejiang, China (Grant No. LY18A040003), the Natural Science Foundation of Ningbo, China (Grant No. 2018A610220), and the K.C. Wong Magna Fund in Ningbo University, China. The computation was performed in the Supercomputer Center of NBU.

†Corresponding author. E-mail: weishihao@nbu.edu.cn

© 2019 Chinese Physical Society and IOP Publishing Ltd

and have poor selectivity of SO_2. To explore catalysts with high activity and favorable SO_2 selectivity is important for the successful reaction. Compared to monometallic clusters, the catalytic bimetallic clusters reveal excellent characteristics, the appropriate modification of the electronic properties will be explored to facilitate the particular catalytic reaction. During CO oxidation, the catalytic activity of the Au_3Cu_1 alloy is enhanced greatly in comparison with monometallic gold,[29] the rate of CO oxidation by the Au–Cu/CeO_2 catalyst is much faster than that by the Au nanocluster of the Au/CeO_2 system,[30] and Au clusters can be air pollutants hunters.[38] The single-atom Au dispersed on solid supports also shows enhancement of activity of some reactions like oxygen evolution reaction (OER)[25] and nitroarene hydrogenation.[26] Apart from the components of catalysts, the charge state is also a key factor that influences the catalytic properties of the catalysts in particular reactions. It was demonstrated that the interaction between charged Au clusters and O_2 is stronger than that between neutral Au clusters and O_2.[39] Wang *et al.* showed that Au_3 anion cluster can select coadsorption complex of CO and O_2.[40] Kelvin Suggs *et al.* also proved that the Au atomic systems in the anionic state are optimal for catalyzing the oxidation of water to peroxide.[41] Zhang *et al.* have shown that Gd doped gold clusters can effectively enhance the catalytic activity of gold clusters.[42]

Although numerous studies have explored the catalytic activity of the Au-based catalysts, there is still no systematic study concerning the reaction of SO_2 reduction by CO over Au-based catalysts published yet, and the research of nano-clusters is a good indication to reveal the catalyst intrinsic property. Here, considering that transition-metal-doped gold clusters have unique catalytic, electronic, and optical properties and Au_5M^n (M = Cu, Ag, Au; $n = 0, -1$) are magic clusters,[43–46] we investigate the catalytic properties of Au_5M^n (M = Ni, Pd, Pt, Cu, Ag, Au; $n = 1, 0, -1$) clusters for the reduction of SO_2 by CO. Based on the design principles of catalysts, we aim at the selectivity and catalytic performance of the catalyst to evaluate its real performance. Comparing the different doping elements in Au clusters and different charged Au_5M clusters, our results show that the charged Au_5Cu^- cluster can not only effectively achieve the selectivity of SO_2, thereby avoiding CO adsorption poisoning, but also improve the catalytic performance.

2. Calculation details

The spin-unrestricted density functional theory (DFT) calculation is performed by using the DMol^3 code[47,48] embedded in the Materials Studio software. The generalized gradient approximation (GGA) with the revised Perdew, Bruke, and Ernzerhof function (RPBE)[49] is used for describing the exchange–correlation interaction. The Kohn–Sham equation is expanded in term of a double-numeric quality basis set plus d-orbit polarization (DND) functions. The all electron relativistic potential is employed to treat the core electron. In addition, the self-consistent field (SCF) calculation is executed with convergence tolerances of 2.0×10^{-5} Ha, 4.0×10^{-3} Ha/Å, and 5.0×10^{-3} Å for the energy, force, and displacement, respectively. The transition-state calculations employ the synchronous transit methods, including the linear and quadratic synchronous transit, in combination with the conjugate gradient minimization algorithm for subsequent refinement.

The adsorption energy (E_{ads}^{ML}) of ML molecule (ML = SO_2, CO, SO, and COS) adsorbed on Au_5M^n and the desorption energy (E_{des}^{ML}) of ML molecule desorbed from Au_5M^n are described as

$$E_{ads}^{ML} = E_{ML+Au_5M^n} - E_{Au_5M^n} - E_{ML}, \quad (1)$$

$$E_{des}^{ML} = -(E_{ML+Au_5M^n} - E_{Au_5M^n} - E_{ML}), \quad (2)$$

where $E_{ML+Au_5M^n}$, $E_{Au_5M^n}$, and E_{ML} represent the total energies of the ML molecule adsorbed on Au_5M^n, the isolated Au_5M^n cluster, and the isolated ML molecule, respectively. It is found that

$$E_{ads}^{ML} = -E_{des}^{ML}. \quad (3)$$

The overall reaction pathway of SO_2 reduction by CO is a multistep chemical process as follows:

$$^*SO_2 + CO \xrightarrow{\text{catalyst}} {}^*SO + CO_2, \quad (4)$$

$$^*SO + CO \xrightarrow{\text{catalyst}} {}^*S + CO_2, \quad (5)$$

$$^*S + CO \xrightarrow{\text{catalyst}} COS^*, \quad (6)$$

where * and X^* denote the adsorption site on the catalyst surface and the adsorbed X species, respectively.

The activation energies for the above three elementary reactions are identified by complete linear synchronous transition and quadratic synchronous transit search methods, following by transition-state optimization and confirmation. The optimized transitional points on the potential energy surface are verified by the second-order derivatives of the energy with respect to the atomic coordinates (Hessian) through vibrational frequency calculations. We take the largest activation energy (E_{act}^{max}) for the three elementary reactions as the overall reaction activation energy. The desorption energy (E_{des}^{COS}) of COS desorbed from the catalyst is another key factor to evaluate the catalyst's property. If $E_{act}^{max} > E_{des}^{COS}$, the catalyst is free from the poisoning, and vice versa.

3. Results and discussion

3.1. Atomic structure for Au_5M^n

Firstly, the equilibrium atomic structures of Au_5M^n (M = Ni, Pd, Pt, Cu, Ag, Au; $n = 1, 0, -1$) clusters are studied. Fig-

ure 1 only shows the most stable (left) and metastable (right) structures for Au_5M and Au_5M^- clusters. As shown in Fig. 1, the most stable structures of the neutral and negative clusters are all planar triangular structures (C_{2v} symmetry) except for Au_5Ni^- and Au_5Pt^-. These results are in accordance with those of previous researches.[50–57] For Au_5Ni^- and Au_5Pt^-, the ground state structures are hexagonal structures lacking a vertex angle atom, and the doped atom (Ni or Pt) is located at the center of the hexagon. It is interesting to find that the metastable structures for Au_5Ni^- and Au_5Pt^- are all planar triangular structures with a C_{2v} symmetry, which have little higher binding energies (about 0.11 eV and 0.08 eV, respectively). Meanwhile, the energy barrier for the structure transition from the hexagonal structure lacking a vertex angle atom to the planar triangular structure is about 0.34 eV and 0.33 eV for Au_5Ni^- and Au_5Pt^-, respectively.

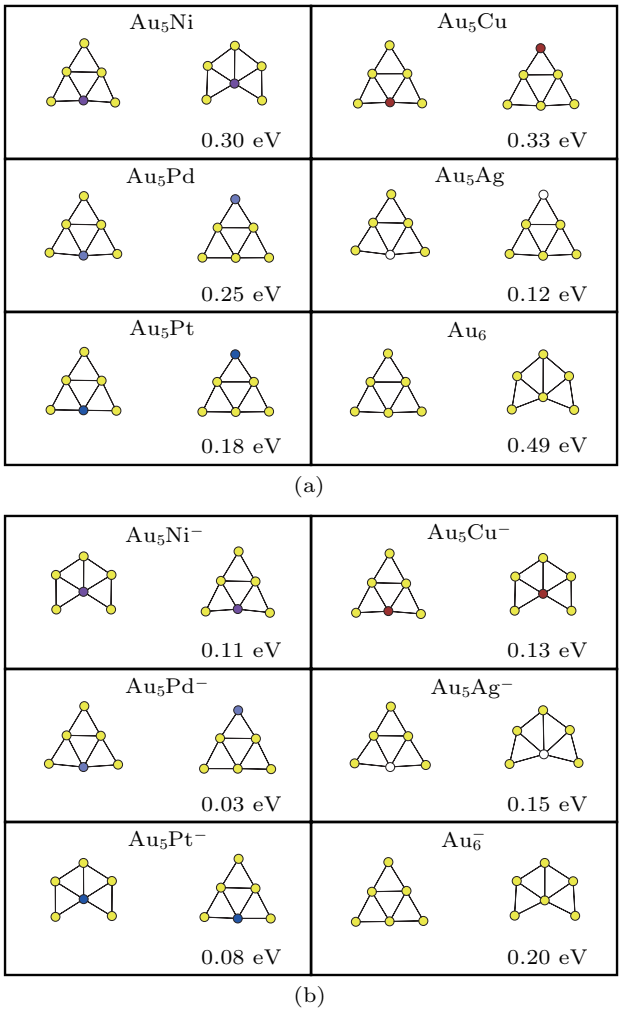


Fig. 1. Equilibrium structures for (a) Au_5M and (b) Au_5M^-. The indigo, bice, blue, brown, silver, and yellow spheres represent nickel, palladium, platinum, copper, silver, and gold atoms, respectively.

3.2. Interaction between clusters and CO, SO_2

In general, SO_2 adsorbed on the catalyst is necessary for the subsequent SO_2 reduction. We also notice that the elemental S is in the solid phase, so it is very important to further reduce the elemental S by CO to the gas phase COS, which can effectively prevent sulfur poisoning. In order to understand the catalytic property, the initial adsorption behavior of the reactant is crucial because the molecules adsorption serves as the foundation for subsequent catalytic reaction. The optimized structures of Au_5M^n-CO and Au_5M^n-SO_2 ($n = 0, -1$) are shown in Fig. 2. The adsorption energy E_{ads}^{ML} of ML molecule absorbed on Au_5M^n in the present calculation is listed in Table 1. The negative sign in front of the numerical value represents an exothermic adsorption. Clearly, as shown in Fig. 2, except for Au_5Ni^-, whether it is a neutral or charged cluster, CO and SO_2 would normally be inclined to bind to the doping atom at the same time when M = Ni, Pd, Pt, and CO and SO_2 would be inclined to bind to the Au atom when M = Cu, Ag, Au. For Au_5Ni^-, SO_2 is adsorbed on Au and Ni atoms simultaneously. Meanwhile, the structure of Au_5Ni^- changes from the hexagonal structure lacking a vertex angle atom to the triangle structure. The structure of Au_5Pt^- also changes from the hexagonal structure lacking a vertex angle atom to the triangle structure when SO_2

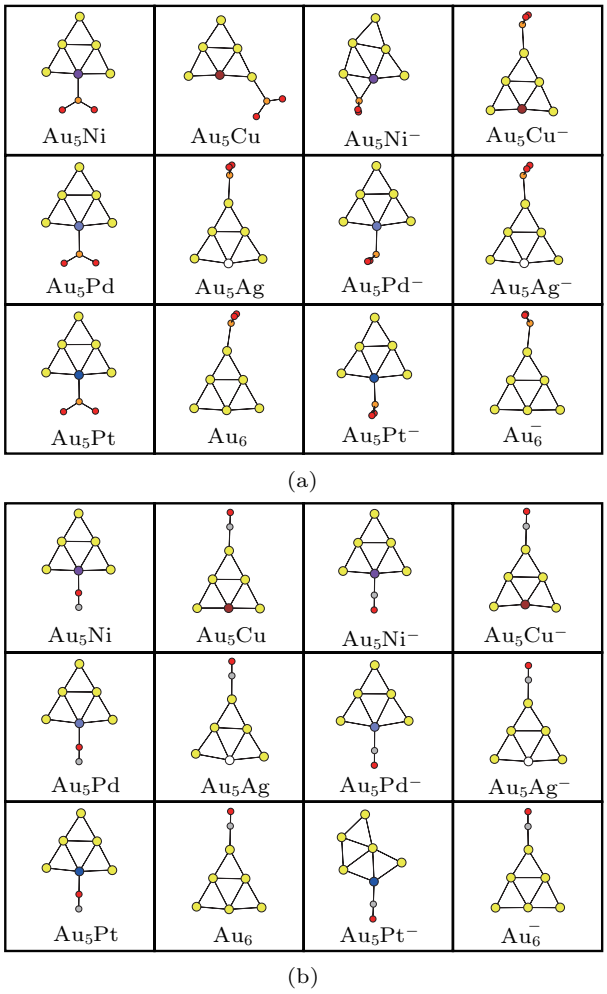


Fig. 2. Equilibrium structures for (a) $(Au_5M\text{-}SO_2)^n$ and (b) $(Au_5M\text{-}CO)^n$ ($n = 0, -1$). The indigo, bice, blue, brown, silver, yellow, grey, red, and orange spheres represent nickel, palladium, platinum, copper, silver, gold, carbon, oxygen, and sulfur atoms, respectively.

is adsorbed on Au_5Pt^-, the same result is found when CO is adsorbed on Au_5Ni^-. However, when CO is adsorbed on Au_5Pt^-, the structure of Au_5Pt^- changes from C_{2v} symmetry to C_s symmetry, meanwhile both of two structures are still hexagonal structure lacking a vertex angle atom, as shown in Figs. 1(b) and 2(b), respectively. Then we can conclude that, whether it is a neutral or anionic cluster, CO or SO_2 would normally be inclined to bind to the doping atom which is a platinum group element (PGE) and to the Au atom which is far away from the doping atom for the dopant of copper family element (CFE), except for Au_5Cu adsorbed SO_2 when CO or SO_2 molecule is adsorbed on the host cluster.

Table 1. Adsorption energy $E_{ads}^{SO_2}$, E_{ads}^{CO}, E_{ads}^{SO}, E_{ads}^{COS} of SO_2, CO, SO, COS absorbed on Au_5M^n, respectively. The negative sign in front of the numerical value represents an exothermic adsorption. Due to $E_{ads}^{SO_2} < E_{ads}^{CO}$ for the positively charged clusters, which means that they will suffer from CO poisoning, so their E_{ads}^{SO} and E_{ads}^{COS} are not shown here.

System	$E_{ads}^{SO_2}$	E_{ads}^{CO}	E_{ads}^{SO}	E_{ads}^{COS}
Au_5Ni	–0.85	–1.36	–1.65	–0.29
Au_5Pd	–0.83	–1.37	–1.84	–0.44
Au_5Pt	–1.54	–2.47	–2.60	–0.81
Au_5Cu	–0.67	–1.37	–1.01	–0.32
Au_5Ag	–0.70	–1.43	–1.03	–0.51
Au_6	–0.64	–1.37	–1.02	–0.46
Au_5Ni^-	–1.74	–1.92	–2.21	–0.68
Au_5Pd^-	–1.64	–1.56	–2.18	–0.74
Au_5Pt^-	–2.10	–2.88	–2.67	–1.03
Au_5Cu^-	–1.79	–1.67	–2.59	–0.73
Au_5Ag^-	–1.80	–1.67	–2.60	–0.76
Au_6^-	–1.72	–1.61	–2.52	–0.66
Au_5Ni^+	–0.62	–1.23	–	–
Au_5Pd^+	–0.96	–1.88	–	–
Au_5Pt^+	–1.76	–3.00	–	–
Au_5Cu^+	–0.69	–1.66	–	–
Au_5Ag^+	–0.65	–1.62	–	–
Au_6^+	–0.68	–1.68	–	–

As shown in Figs. 1(b) and 2(b), the structure of Au_5Ni^- cluster would deform and change from hexagonal structure lacking a vertex angle atom to planar triangular structure when Au_5Ni^- adsorbs SO_2 (or CO) molecule, simultaneously, the structure of Au_5Pt^- cluster also changes very obviously when SO_2 (or CO) molecule adsorbs on the cluster. We find that, when SO_2 (or CO) molecule is removed from Au_5Ni^- and Au_5Pt^- clusters, the stable structure of the cluster will become a planar triangular structure which is the metastable structure of the Au_5Ni^- or Au_5Pt^- cluster, rather than a hexagonal structure lacking a vertex angle atom which is the most stable structure of the Au_5Ni^- or Au_5Pt^- cluster. It is due to that, when SO_2 (or CO) molecule is adsorbed on the Au_5Ni^- or Au_5Pt^- cluster, it is an exothermic reaction in which the heat released is about 1.74 eV (or 2.10 eV), at the same time, the structure transition from the ground state structure to the metastable structure is an endothermic process which is about 0.34 eV (0.33 eV) for the Au_5Ni^- (Au_5Pt^-) cluster. So when SO_2 (or CO) is adsorbed onto the Au_5Ni^- or Au_5Pt^- cluster, the energy released is enough to make the structure of the host cluster to change from the ground state structure to the metastable structure, as shown in Figs. 1 and 2. In the subsequent catalytic reaction, we use their metastable structure as a reaction initial configuration.

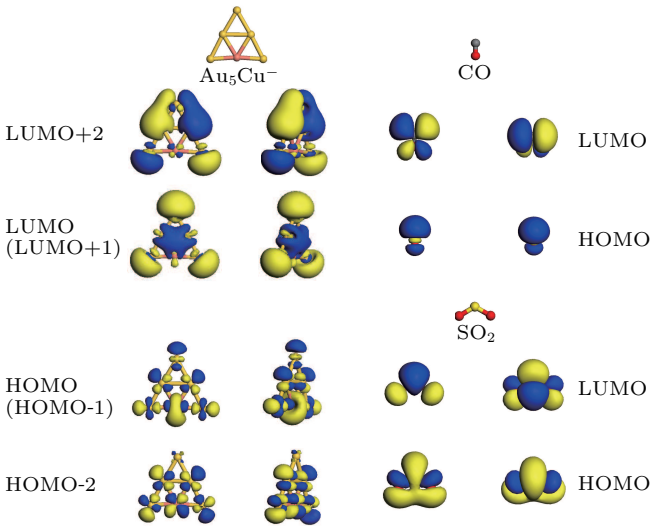


Fig. 3. The frontier molecular orbitals (isosurface value = 0.02) of the Au_5Cu^- cluster, CO, and SO_2. HOMO, HOMO-1, HOMO-2 and LUMO, LUMO+1, LUMO+2 represent the highest, second highest, and third highest occupied molecular orbitals and the lowest, second lowest, and third lowest unoccupied molecular orbitals, respectively. Moreover, HOMO and HOMO-1, LUMO, and LUMO+1 are degeneration orbitals. The second column is the first column turned 30° along the vertical axis, and the fourth column is the third column rotated 30° along the horizontal axis. The brown, yellow, grey, red, and golden spheres represent copper, gold, carbon, oxygen, sulfur, respectively.

It is well established that the frontier molecular orbitals (FMOs) are very critical for identifying the adsorption sites of small molecules on small metal clusters. According to this point, we can explain very well the change of adsorption position of the adsorbed molecules (SO_2 and CO) when the cluster is charged, as shown in Fig. 2. For the sake of simplicity, we only take the Au_5Cu^- cluster as an example to illustrate this phenomenon. Figure 3 shows the FMOs (isosurface value = 0.02) of the Au_5Cu^- cluster, CO, and SO_2. HOMO, HOMO-1, HOMO-2, and LUMO, LUMO+1, LUMO+2 represent the highest, second highest, and third highest occupied molecular orbitals and the lowest, second lowest, and third lowest unoccupied molecular orbitals, respectively. Moreover, HOMO and HOMO-1 are degeneration orbitals, and the same with LUMO and LUMO+1. The second column is the first column turned 30° along the vertical axis, and the fourth column is the third column rotated 30° along the horizontal axis. Considering the orbital symmetry matching and electron cloud density matching, the higher the symmetry matching is, the stronger

the interaction is, and the adsorption sites are also located at the position where the electron cloud density is the highest. As shown in Fig. 3, the HOMO and LUMO of SO_2 and CO molecules mainly locate at the sulfur site and carbon site, respectively, which is why C atom of CO and S atom of SO_2 are the adsorption sites of the adsorbed CO and SO_2 molecules. When CO (or SO_2) is adsorbed on Au_5Cu^-, the HOMO of CO (or SO_2) interacts with the LUMO and LUMO+1 of Au_5Cu^- according to the matching of symmetry and electron cloud density, while the HOMOs (including HOMO-1 and HOMO-2) of Au_5Cu^- interact with the LUMO of CO (or SO_2) according to the matching of symmetries. So we get the most stable structure of Au_5Cu^-CO and $Au_5Cu^-SO_2$ (shown in Fig. 2).

As shown in Table 1, for the neutral Au_5M clusters, we can find that $E_{ads}^{SO_2}$ is always smaller than E_{ads}^{CO}. This means that, when SO_2 and CO molecules are adsorbed onto the clusters simultaneously, CO will preferentially adsorb onto the Au_5M clusters, which shows that the catalytic efficiency will be significantly reduced. Especially in the case of CO enrichment, SO_2 is basically unable to adsorb onto the host clusters, which indicates that the catalysts Au_5M are poisoned by CO and the reaction for the reduction of SO_2 by CO can not be carried out. The same results are observed for the positively charged clusters, so we do not consider the following reaction for Au_5M^+. When the host Au_5M clusters have a negative charge, it is interesting to find that $E_{ads}^{SO_2}$ is larger than E_{ads}^{CO} except for Au_5Ni^- and Au_5Pt^-, which means that catalysts CO poisoning can be avoided effectively. It is due to the fact that the different electronic configurations of nickel ($[Ar]3d^84s^2$) and platinum ($[Xe]4f^{14}5d^96s^1$) in which the d-orbital is partially occupied would remodel the electronic structure when SO_2 or CO molecule is adsorbed onto the host cluster. As a consequence, when Au_5M (M = Cu, Ag, Au, Pd) clusters have a negative charge, it could improve the selectivity of SO_2 for the host clusters and avoid the catalyst CO poisoning simultaneously.

In order to understand the change of the adsorption energies, $E_{ads}^{SO_2}$ and E_{ads}^{CO} of SO_2 and CO on the corresponding charged clusters, we calculate the charge transfer between the clusters and adsorbed molecules (SO_2 or CO) according to the Mulliken charges population (MCP). Table 2 shows the charge transfer between the adsorbed molecule and the corresponding cluster. As can be seen from Table 2, when SO_2 or CO is adsorbed on the Au_5M^+ cluster, the charge transfer of CO is always larger than that of SO_2, so E_{ads}^{CO} is always bigger than $E_{ads}^{SO_2}$ for Au_5M^+ (as shown in Table 1). It is due to that the more charge transfer between the adsorbed molecule and the corresponding cluster, the stronger interaction between them. So E_{ads}^{CO} is always larger than $E_{ads}^{SO_2}$ for Au_5M^+. For the neutral Au_5M clusters, although adsorbed SO_2 has more net charge than adsorbed CO for Au_5M (M = Ni, Pd), it should be pointed out that the bonding between CO and transition metal clusters abide by Blyholder model which is the σ non-bonding orbital of CO can transfer electrons to the empty orbital of the transition metal clusters, and the π antibonding orbital of CO also can accept the electrons from the occupied orbital of the transition metal clusters (back donation),[58] indicating that the net charges of CO are not equal to the total quantity of electrons transferred between CO and catalysts, so E_{ads}^{CO} is still bigger than $E_{ads}^{SO_2}$ for the neutral Au_5M clusters. However, these unfavorable outcome will be improved when Au_5M carries a negative electron. As can be seen from Table 2, numbers of electrons transferred from Au_5M^- to SO_2 are much larger than those of Au_5M^- to CO, especially for Au_5M^- (M = Cu, Ag, Au), so $E_{ads}^{SO_2}$ becomes greater than E_{ads}^{CO}, except for Au_5Pt^- and Au_5Ni^-. For Au_5Pt^-, the net charge transfer (0.274) from Au_5Pt^- to SO_2 is a little larger than that (0.115) of Au_5Pt^- to CO, but due to the fact that the charge transfer between CO and transition metal clusters abide by Blyholder model, which may make that the net charges transfer from Au_5Pt^- to CO are little more than that of Au_5Pt^- to SO_2, so E_{ads}^{CO} (2.88 eV) becomes larger than $E_{ads}^{SO_2}$ (2.10 eV) for Au_5Pt^- (as shown in Table 1). The same result is found when CO and SO_2 are adsorbed on Au_5Ni^-.

Table 2. The charge transfer between adsorbed molecules and Au_5M^n clusters. Plus sign represents that the adsorbed gas donates electrons to the clusters, and minus sign represents that the adsorbed gas accepts electrons from the clusters.

Adsorbed gas	Au_5Ni^+	Au_5Pd^+	Au_5Pt^+	Au_5Ni	Au_5Pd	Au_5Pt	Au_5Ni^-	Au_5Pd^-	Au_5Pt^-
CO	+0.283	+0.108	+0.216	–0.002	+0.009	+0.069	–0.166	–0.157	–0.115
SO_2	+0.219	+0.011	+0.169	–0.149	–0.074	–0.044	–0.368	–0.398	–0.274

Adsorbed gas	Au_5Cu^+	Au_5Ag^+	Au_6^+	Au_5Cu	Au_5Ag	Au_6	Au_5Cu^-	Au_5Ag^-	Au_6^-
CO	+0.297	+0.281	+0.289	+0.157	+0.154	+0.157	–0.069	–0.069	–0.066
SO_2	+0.240	+0.231	+0.242	–0.038	+0.033	+0.012	–0.399	–0.408	–0.402

Figure 4 shows the average bond-length between sulfur atom and oxygen atom ($R_{S-O}^{SO_2}$) and the Mulliken charge population (MCP) of SO_2 when the SO_2 molecule is adsorbed onto Au_5M^n cluster. The Mulliken charge population analysis shows that SO_2 is an electron acceptor when SO_2 absorbs onto the neutral Au_5M (M = Ni, Pd, Pt, Cu) cluster except for neutral Au_5Ag and Au_6 clusters. Compared with the neutral Au_5M cluster, the net charge of SO_2 increases when the SO_2 molecule is adsorbed onto Au_5M^- cluster. But the net charge of SO_2 is always smaller than 0.5, as shown in Fig. 4. We notice that when SO_2 is adsorbed onto negative charged Au_5M cluster, the charge of the $(Au_5MSO_2)^-$ cluster will be redistributed, which means that this electron belongs to the whole cluster (Au_5MSO_2). It indicates that the net charge of the Au_5M cluster is greater than that of SO_2. It is precisely because more electrons transfer to SO_2 from Au_5M^- (M = Cu, Ag, Au) clusters, Au_5M^- have a surge of adsorption capacity. For SO_2 adsorbed onto Au_5M^- cluster, the more net charge of SO_2, the stronger the mutual dismantling force between the sulfur atom and oxygen atom, which will lead to the S–O bond-length becoming longer. It is precisely because more electrons transfer to SO_2 from Au_5M^- (M = Cu, Ag, Au) clusters, Au_5M^- have a surge of adsorption capacity. So $E_{ads}^{SO_2}$ of Au_5M^- is much greater than that of Au_5M (shown in Table 1). As shown in Fig. 4, the change of the S–O bond-length is in accordance with the change of the net charge of SO_2, which confirms this conclusion. For Au_5Cu^-, Au_5Ag^-, and Au_6^-, the net charge curve is above the d_{S-O} curve, which is due to that the total magnetic moments of the Au_5M^- (M = Cu, Ag, Au) clusters are $1\mu_B$ and at the same time the magnetic moments of other Au_5M^n (M = Ni, Pd, Pt, Cu, Ag, Au; n = 0, 1) clusters are $0\mu_B$. The longer the S–O bond-length, the weaker the interaction between the S atom and O atom, which means that the reduction of SO_2 by CO with Au_5M^n clusters acting as a gas catalyst is easier to carry out. It is anticipated that the longer $R_{S-O}^{SO_2}$ is in a position to lower the reaction barrier for the reduction of SO_2 by CO.

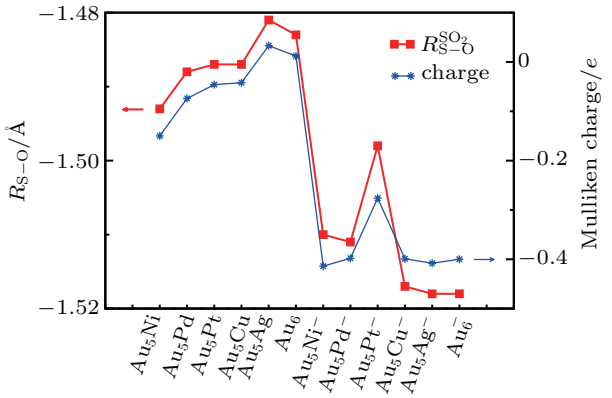


Fig. 4. The average bond-length between sulfur atom and oxygen atom ($R_{S-O}^{SO_2}$) and the Mulliken charge (MC) of SO_2 adsorbed onto Au_5M^n clusters.

3.3. Reduction of SO_2 by CO with Au_5M^n clusters

Understanding the reaction mechanisms of the reduction of SO_2 by CO with Au_5M^n clusters is essential for enhancing the performance of the catalysts. We next investigate the Eley–Rideal (ER) mechanism as the starting point to study the catalytic reaction pathway and take the Au_5Cu^- cluster as an example to illustrate the whole process of catalytic reaction. The energy profiles for the reduction of SO_2 by CO over Au_5Cu^-, the structures of the reactants, transition states, and products are shown in Fig. 5. The energies of the intermediates, transition states, and products are related to the energy of the entrance (including the free catalyst, one isolated SO_2 molecule, and three isolated CO molecules, and the entrance is set to zero). The changes of the energies for the reduction of SO_2 by CO to COS over the Au_5M^n clusters are shown in Table 3, and the corresponding catalytic reaction pathways of others Au_5M^n catalysts are exactly the same as that of the Au_5Cu^- cluster (shown in Fig. 5). We take the largest activation energy (E_{act}^{max}) for the three elementary reactions as the overall reaction's activation energy and the numbers in italics represent E_{act}^{max} (shown in Table 3).

For the first step of reaction $^*SO_2 + CO \xrightarrow{\text{catalyst}} {}^*SO + CO_2$, firstly the SO_2 molecule is chemically adsorbed onto the optimized Au_5Cu^- cluster, and then a CO molecule is physically adsorbed to the $Au_5CuSO_2^-$, thus the intermediate $^*SO_2$+ CO (IM1) is formed. As shown in Fig. 5, the IM1 locates below the entrance by 1.87 eV. Next, the first O atom of $^*SO_2$ will interact with the CO molecule to form transition state TS12 with a barrier of 1.16 eV. This O atom is being activated and combined with the CO molecule to form a CO_2 molecule, in which the intermediate $^*SO + CO_2$ (IM2) is the complex of Au_5CuSO^- with a CO_2 molecule. The total energy of IM2 is below the entrance by 3.28 eV. Finally, CO_2 is released into the atmosphere.

The second step of reaction is $^*SO + CO \xrightarrow{\text{catalyst}} {}^*S + CO_2$. The second physisorbed CO molecule is introduced for the rest of IM2 to form the intermediate $^*SO$ + CO (IM3). This CO molecule binds with the second O atom of the SO_2 molecule to form the second CO_2 molecule and the intermediate $^*S + CO_2$ (IM4) is formed, which consists of Au_5CuS^- and a dissociative CO_2 molecule. IM3 converts into IM4 via transition state TS34 with a barrier of 0.77 eV.

Finally, the third step of reaction is $^*S + CO \xrightarrow{\text{catalyst}} COS^*$. Now the third physisorbed CO molecule is imported to form the intermediate $^*S$ + CO (IM5), and then CO molecule binds with the sulfur atom to form the intermediate COS^* (IM6) through transition state TS56 with a barrier of 0.06 eV. IM6 dissociates directly to the COS molecule and catalyst (Au_5Cu^-), indicating the accomplishment of the reaction. The E_{des}^{COS} is about 0.73 eV.

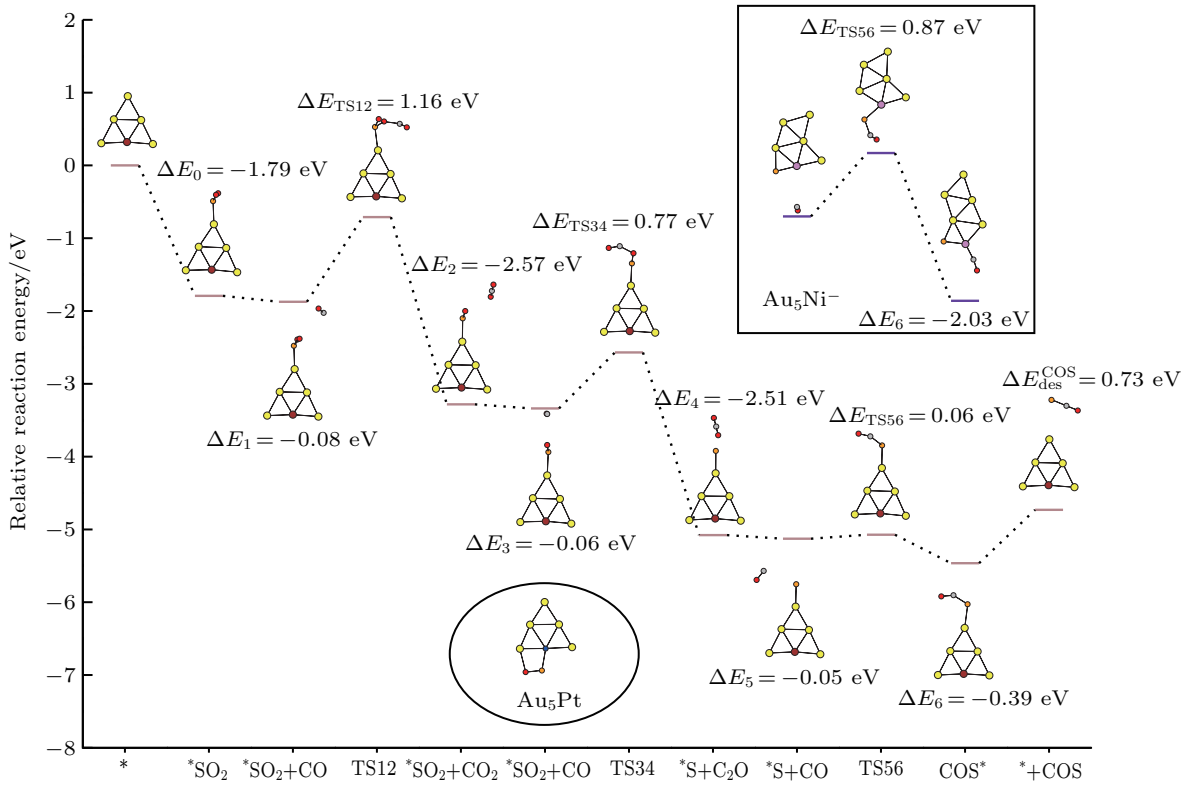


Fig. 5. Energy profile for reduction of SO_2 by CO with Au_5Cu^- cluster. The brown, yellow, grey, red, orange, blue, and indigo spheres represent copper, gold, carbon, oxygen, sulfur, platinum, and nickel atoms, respectively. The rectangle figure shows that, for Au_5Ni^-, S, and CO cannot be combined into COS molecule in the third step of reaction. The ellipse figure shows that, for Au_5Pt, SO molecule lies flat on the Pt–Au (or Pt–Ni) bond in the second elementary step, resulting in a strong combination of SO and Au_5Pt (or Au_5Ni) cluster.

It is worth noting that all the whole processes of catalytic reaction for the reduction of SO_2 by CO to COS with Au_5M^n (M = Ni, Pd, Pt, Cu, Ag, Au; $n = 0, -1$) can be divided into three elementary reactions, and all reactions can proceed smoothly, just like Au_5Cu^- (as shown in Fig. 5), except for Au_5Ni^-. For Au_5Ni^-, the first and second steps of the reaction can still be carried out smoothly, but COS can not be formed and desorbed from Au_5Ni^- in the third step of reaction (as shown in Table 3). It is due to that the sulfur atom is combined with Au atom and Ni atom simultaneously, at the same time, CO is bound to the Ni atom and far away from the sulfur atom (as shown in the rectangle of Fig. 5), which results in that S and CO cannot be combined into COS molecule.

As shown in Table 3, we notice that PGE doping (including Ni doping) has a lower ΔE_{TS12} (about 1.32 eV, 1.35 eV, and 1.31 eV for Au_5Ni, Au_5Pd, and Au_5Pt, respectively) than CFE doping for neutral Au_5M. This is due to that the PGE doping (including Ni doping) has a relatively larger $E_{ads}^{SO_2}$ and longer $R_{S-O}^{SO_2}$ when SO_2 is adsorbed onto the neutral Au_5M clusters. The greater the adsorption energy $E_{ads}^{SO_2}$, the smaller the activation energy ΔE_{TS12}.[58] The longer the bond-length $R_{S-O}^{SO_2}$, the weaker the bond energy of the S–O bond, and the higher the activity of the oxygen atom of the SO_2 molecule, the smaller the activation energy ΔE_{TS12}. It is worth noting that $E_{ads}^{SO_2}$ of Au_5Cu, Au_5Ag, and Au_6 are almost the same, but their ΔE_{TS12} are quite different (1.64 eV, 1.80 eV, and 1.76 eV for Au_5Cu, Au_5Ag, and Au_6, respectively). This is because the SO_2 molecule has a net positive charge when it is adsorbed onto Au_5Ag and Au_6 (shown in Fig. 4), causing the $R_{S-O}^{SO_2}$ to be shorter than that in isolated SO_2. When Au_5M has an electron on it, for SO_2 adsorbed onto Au_5M^-, $E_{ads}^{SO_2}$ can be greatly improved (by about 1 eV), at the same time, ΔE_{TS12} for the CFE doping Au_5M^- (M = Cu, Ag, Au) clusters decreases from (1.64 eV, 1.80 eV, 1.76 eV) to (1.16 eV, 1.17 eV, 1.18 eV), as shown in Table 3. It is due to that they have not only greater $E_{ads}^{SO_2}$, but more importantly, longer $R_{S-O}^{SO_2}$ (shown in Fig. 4). The longer $R_{S-O}^{SO_2}$ indicates that the activity of SO_2 is improved. The present results also suggest that $E_{ads}^{SO_2}$ and $R_{S-O}^{SO_2}$ jointly determine the first reaction barrier for the reduction of SO_2 by CO over Au_5M^n clusters, but the effect of $R_{S-O}^{SO_2}$ on the barrier is more important than that of $E_{ads}^{SO_2}$.

It is worth noting that the competition between the desorption of SO_2 molecule and the reaction of SO_2 reduction by CO to SO over Au_5M^n clusters also has an important influence on the catalytic reaction. The desorption energy ($E_{des}^{SO_2}$) of SO_2 molecule desorbed from Au_5M^n clusters and the potential barrier (ΔE_{TS12}) of the reduction of SO_2 by CO to SO over Au_5M^n clusters are depicted in Fig. 6. Clearly, for the neutral Au_5M clusters, $E_{des}^{SO_2}$ is smaller than ΔE_{TS12} except for Au_5Pt, and for the charged Au_5M^- clusters, $E_{des}^{SO_2}$ is always greater than ΔE_{TS12}. It indicates that, for the first step reaction $^*SO_2 + CO \xrightarrow{\text{catalyst}} {}^*SO + CO_2$, the reaction always proceeds in the positive direction if $E_{des}^{SO_2} > \Delta E_{TS12}$, and vice versa.

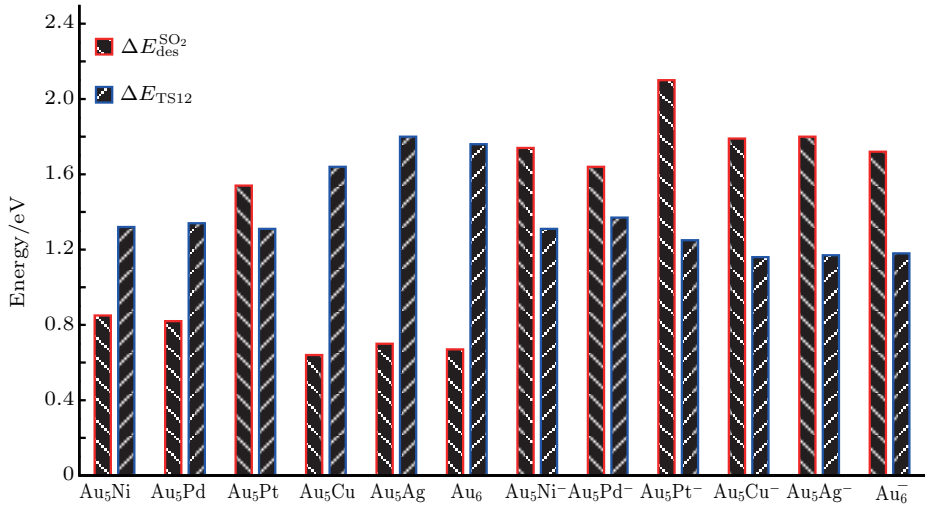


Fig. 6. The desorption energy ($E_{\rm des}^{\rm SO_2}$) of SO_2 molecule desorbed from Au_5M^n clusters and the potential barrier ($\Delta E_{\rm TS12}$) of the reduction of SO_2 by CO to SO over Au_5M^n clusters.

Similarly, the competition between the desorption of SO molecule and the reaction of SO reduction by CO over Au_5M^n clusters also has an important influence on the second step of reaction $^*{\rm SO}+{\rm CO}\xrightarrow{\rm catalyst}{}^*{\rm S}+{\rm CO_2}$. $E_{\rm ads}^{\rm SO}$ ($E_{\rm ads}^{\rm SO}=-E_{\rm des}^{\rm SO}$, see Eq. (3)) and $E_{\rm ads}^{\rm COS}$ are listed in Table 1, and the bond length between sulfur atom and oxygen atom ($R_{\rm S-O}^{\rm SO}$) of SO adsorbed onto Au_5M^n clusters and the potential barrier ($\Delta E_{\rm TS34}$) of the reduction of SO by CO to S over Au_5M^n clusters are shown in Fig. 7. $\Delta E_{\rm TS34}$ is also given in Table 3. The desorption energy ($E_{\rm des}^{\rm SO}$) of SO molecule desorbed from Au_5M^n clusters and the potential barrier ($\Delta E_{\rm TS34}$) of the reduction of SO by CO to S over Au_5M^n clusters are depicted in Fig. 8. Just like the relationship between $E_{\rm ads}^{\rm SO_2}$ and $\Delta E_{\rm TS12}$, we also find that $E_{\rm ads}^{\rm SO}$ and $\Delta E_{\rm TS34}$ have the same relationship. In other words, for the neutral and charged Au_5M clusters, the smaller the $E_{\rm ads}^{\rm SO}$, the higher the $\Delta E_{\rm TS34}$, and vice versa. From Fig. 7, the variation tendency of $\Delta E_{\rm TS34}$ is exactly the same as that of $R_{\rm S-O}^{\rm SO}$ except for Au_5Pt, which means that the longer the bond length $R_{\rm S-O}^{\rm SO_2}$, the smaller the activation energy, and vice versa. For the neutral Au_5Pt cluster adsorbed SO molecule, the SO molecule lies flat on the Pt–Au bond, resulting in a strong combination of SO and Au_5Pt cluster, as shown in the ellipse of Fig. 5. Therefore, the reaction of this step requires more energy (about 1.38 eV, as shown in Table 3).

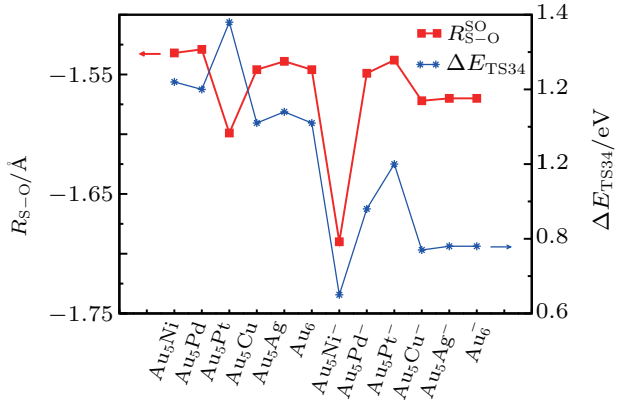


Fig. 7. The bond length between sulfur atom and oxygen atom ($R_{\rm S-O}^{\rm SO}$) of SO adsorbed onto Au_5M^n clusters and the potential barrier ($\Delta E_{\rm TS34}$) of the reduction of SO by CO to S over Au_5M^n clusters.

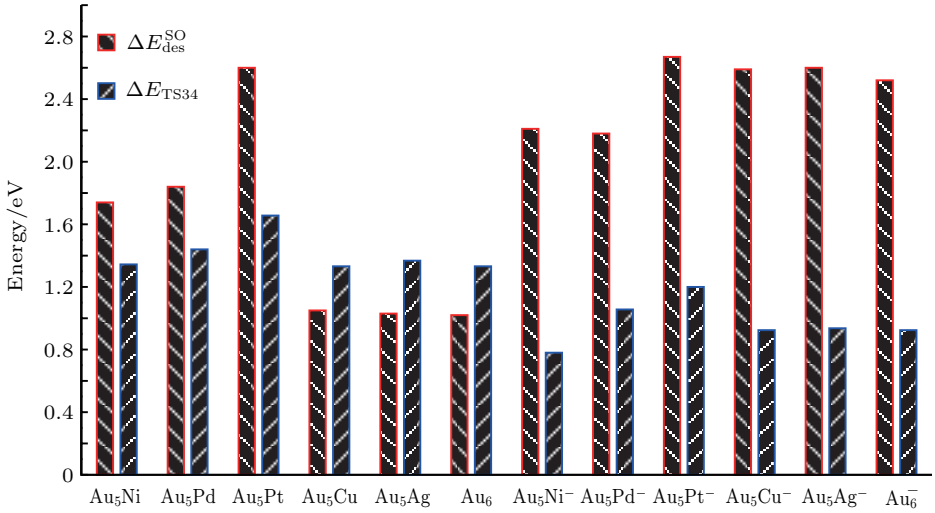


Fig. 8. The desorption energy ($E_{\rm ads}^{\rm SO}$) of SO molecule desorbed from Au_5M^n clusters and the potential barrier ($\Delta E_{\rm TS34}$) of the reduction of SO by CO to S over Au_5M^n clusters.

Table 3. The change of the energies (in eV) for the reduction of SO_2 by CO to COS over the Au_5M^n clusters. We take the largest activation energy (E_{act}^{max}) for the three elementary reactions as the overall reaction activation energy. The numbers in italics represent the E_{act}^{max}, and absolute value of ΔE_0 equals $E_{ads}^{SO_2}$ (shown in Table 1).

System	ΔE_0	ΔE_1	ΔE_{TS12}	ΔE_2	ΔE_3	ΔE_{TS34}	ΔE_4	ΔE_5	ΔE_{TS56}	ΔE_6	ΔE_{des}^{COS}
Au_5Ni	–0.85	–0.06	*1.32*	–2.81	–0.04	1.22	–3.37	–0.05	0.60	–0.97	0.29
Au_5Pd	–0.83	–0.03	*1.35*	–2.99	–0.02	1.20	–3.05	–0.06	0.38	–1.10	0.44
Au_5Pt	–1.54	–0.06	1.31	–2.96	–0.04	*1.38*	–3.11	–0.06	0.58	–1.03	0.81
Au_5Cu	–0.67	–0.05	*1.64*	–2.64	–0.04	1.11	–2.61	–0.04	0.12	–1.88	0.32
Au_5Ag	–0.70	–0.04	*1.80*	–2.73	–0.06	1.14	–2.63	–0.05	0.06	–2.03	0.51
Au_6	–0.64	–0.05	*1.76*	–2.78	–0.05	1.11	–2.70	–0.06	0.14	–1.91	0.46
Au_5Ni^-	–1.74	–0.08	*1.29*	–2.60	–0.03	0.65	–2.93	–0.44	0.87	–2.03	–
Au_5Pd^-	–1.64	–0.09	*1.31*	–2.78	–0.03	0.88	–2.69	–0.05	0.20	–0.90	0.74
Au_5Pt^-	–2.10	–0.08	*1.22*	–2.45	–0.02	1.00	–2.80	–0.01	0.30	–0.87	1.03
Au_5Cu^-	–1.79	–0.08	*1.16*	–2.57	–0.06	0.77	–2.51	–0.05	0.06	–0.39	0.73
Au_5Ag^-	–1.80	–0.09	*1.17*	–2.58	–0.04	0.78	–2.51	–0.06	0.05	–0.41	0.76
Au_6^-	–1.72	–0.09	*1.18*	–2.61	–0.02	0.77	–2.53	–0.03	0.05	–0.40	0.66

It is well known that the excellent properties of catalysts depend on the energy barrier at the rate limiting step. The smaller the energy barrier at the rate limiting step, the faster the reaction process. The largest activation energy (E_{act}^{max}, in italics) for the three elementary reactions and the desorption energy of product COS (E_{des}^{COS}) are listed in Table 3. We take the E_{act}^{max} as the energy barrier at the rate limiting step in this work. It is found that the first elementary step is the rate-determining step for catalysts in both negative charge and neutral states except for the neutral Au_5Pt. For Au_5Pt, the second elementary step is the rate-determining step, which is due to the fact that the SO molecule lies flat on the Pt–Au bond (as shown in the ellipse of Fig. 5), resulting in a strong combination of SO and Au_5Pt cluster. At the same time, for the neutral Au_5M clusters, $E_{ads}^{SO_2}$ ($E_{ads}^{SO_2} = -\Delta E_0$) is always smaller than E_{act}^{max} except for Au_5Pt, and for the charged Au_5M^{-1} clusters, $E_{ads}^{SO_2}$ is always greater than E_{act}^{max}. This means that, by giving a negative charge to the catalyst, the reaction for the reduction of SO_2 by CO always proceeds in the positive direction. So we can conclude that the reaction rate is greatly improved when Au_5M clusters are charged.

4. Conclusion

In summary, using first-principles calculation, we have investigated the equilibrium structures of Au_5M^n (M = Ni, Pd, Pt, Cu, Ag, Au; $n = 1, 0, -1$) clusters without or with adsorbed SO_2 or CO molecule and their catalytic performance for highly selective reduction of SO_2 by CO. The most stable geometrical structures of the Au_5M^n clusters are all planar triangular structures except for Au_5Ni^- and Au_5Pt^- clusters. The most stable adsorption site of the ML (ML = SO_2, CO, SO, and COS) molecule on the catalysts is the top of the doping atom which is a platinum group element (including Ni doping) and the top of the Au atom which is far away from the doping atom for the dopant of the copper family element except for Au_5Cu adsorbed SO_2, which can be explained very well by the match of orbitals symmetry and density of electron cloud through their frontier molecular orbitals. It is interesting to find that, for the neutral Au_5M clusters, $E_{ads}^{SO_2}$ is always smaller than E_{ads}^{CO}, and for the charged Au_5M^- clusters except for Au_5Ni^- and Au_5Pt^-, $E_{ads}^{SO_2}$ is always greater than E_{ads}^{CO}. This means that, by giving a negative charge to the Au_5M (M = Cu, Ag, Au, Pd) clusters, it could improve the selectivity of SO_2 and effectively avoid catalyst CO poisoning simultaneously. At the same time, the reaction rate is greatly improved when the Au_5M clusters are charged. These advantages can be well explained by the charge transfer between clusters and adsorbed molecules. Considering the catalyst cost (Cu is much cheaper than Ag and Au), selectivity of SO_2 which effectively overcomes the catalyst CO poisoning, we propose that Au_5Cu^- is an ideal catalyst for getting rid of SO_2 and CO simultaneously.

References

[1] Kennes C and Veiga M C 2001 *Fundamentals of Air Pollution* (Vol. 4) (Dordrecht: Springer) pp. 3–15
[2] Bao H, Yu S and Tong D Q 2010 *Nature* **465** 909
[3] Li Y R and Gibson J M 2014 *Environ. Sci.Technol.* **48** 10019
[4] Chiang T Y, Yuan T H, Shie R H, Chen C F and Chan C C 2016 *Environ. Int.* **96** 1
[5] Ishiguro A, Nakajima T, Iwata T, Fujita M, Minato T, Kiyotaki F and Matsui Y 2002 *Chem. Eur. J.* **8** 3260
[6] Paik S C, Kim H and Chung J S 1997 *Catal. Today* **38** 193
[7] Liu W, Sarofim A F and Flytzani-Stephanopoulos M 1994 *Appl. Catal. B: Environ.* **4** 167
[8] Zhu T, Kundakovic L, Dreher A and Flytzani-Stephanopoulos M 1999 *Catal. Today* **50** 381
[9] Sarlis J and Berk D 1988 *Ind. Eng. Chem. Res.* **27** 1951
[10] Humeres E, Peruch M G B, Moreira R F P M and Schreiner W 2003 *J. Phys. Org. Chem.* **16** 824
[11] Wang X, Wang A, Wang X and Zhang T 2007 *Energy Fuels* **21** 867
[12] Wang X, Wang A, Li N, Wang X, Liu Z and Zhang T 2006 *Ind. Eng. Chem. Res.* **45** 4582
[13] Gao G P, Wei S H and Duan X M 2012 *J. Phys. Chem. C* **116** 24930
[14] Lau N T, Fang M, Chan C K 2007 *J. Catal.* **245** 301
[15] Liu W, Sarofim A F and Flytzani-Stephanopoulos M 1994 *Appl. Catal. B: Environ.* **4** 167
[16] Lemons R A 1990 *J. Power Sources* **29** 251
[17] Hammer B and Nørskov J K 1995 *Nature* **376** 238

[18] Haruta M, Kobayashi T, Sano H and Yamada N 1987 *Chem. Lett.* **16** 405
[19] Tsubota S, Cunningham D A H, Bando Y and Haruta M 1995 *Stud. Surf. Sci. Catal.* **91** 227
[20] Haruta M 1997 *Catal. Today* **36** 153
[21] Haruta M 1997 *Catal. Surv. Asia* **1** 61
[22] Haruta M 2003 *Chem. Record* **3** 75
[23] Valden M, Lai X and Goodman D W 1998 *Science* **281** 1647
[24] Chen S, Luo L, Jiang Z and Huang W 2015 *ACS Catalysis* **5** 1653
[25] Zhang J, Liu J, Xi L, Yu Y, Chen N, Sun S, Wang W, M.Lange K and Zhang B 2018 *J. Am. Chem. Soc.* **140** 3876
[26] Wang L, Guan E, Zhang J, Yang J, Zhu Y, Han Y, Yang M, Cen C, Fu G, C.Gates B and Xiao F 2018 *Nat. Commun.* **9** 1362
[27] Martirez J. M. P and Carter E. A 2016 *ACS Nano* **10** 2940
[28] Ma J, Gong H, Zhang T, Yu H, Zhang R, Liu Z, Yang G, Sun H, Tang S and Qiu Y 2019 *Appl. Sur. Sci.* **488** 1
[29] Liu X, Wang A, Li L, Zhang T, Mou C Y and Lee J F 2011 *J. Catal.* **278** 288
[30] Zhang L, Kim H Y and Henkelman G 2013 *J. Phys. Chem. Lett.* **4** 2943
[31] Roldán A, González Gonzalez S, Ricart J M and Illas F 2009 *Chem. Phys. Chem.* **10** 348
[32] Lyalin A and Taketsugu T 2010 *J. Phys. Chem. Lett.* **1** 1752
[33] Shekhar M, Wang J, Lee W S, Williams W D, Kim S M, Stach E A, Miller J T, Delgass W N, Ribeiro F H 2012 *J. Am. Chem. Soc.* **134** 4700
[34] Yao S, Zhang X, Zhou W, Gao R, Xu W, Ye Y, Lin L, Wen X, Liu P and Chen B 2017 *Science* **357** 389
[35] Prati L and Rossi M 1998 *J. Catal.* **176** 552
[36] Tsunoyama H, Sakurai H, Negishi Y and Tsukuda T 2005 *J. Am. Chem. Soc.* **127** 9374
[37] Liu H, Liu Y, Li Y, Tang Z and Jiang H 2010 *J. Phys. Chem. C* **114** 13362
[38] Reina M and Martínez A 2018 *Comput. Theor. Chem.* **1130** 15
[39] Okumura M, Kitagawa Y, Haruta M and Yamaguchi K 2005 *Appl. Catal. A General* **291** 37
[40] Wang Z Y, Zhang T L, Li Q H, Xue Q and Wang R 2016 *Comput. Theor. Chem.* **1085** 75
[41] Suggs K, Kiros F, Tesfamichael A, Felfli Z 2015 *J. Phys: Conference Series* **635** 052018
[42] Zhang H X, Hu C H, Wang D H, Zhong Y, Zhou H Y, and Rao G H 2018 *Chin. Phys. B* **27** 083601
[43] Wang H Q, Kuang X Y and Li H F 2010 *Phys. Chem. Chem. Phys.* **12** 5156
[44] Zhang M, He L M, Zhao L X, Feng X J and Luo Y H 2009 *J. Phys. Chem. C* **113** 6491
[45] Guo J J, Wei C F, Yang J X and Die D 2010 *Chin. Phys. B* **19** 113601
[46] Zhang M, Feng X J, Zhao L X, He L M and Luo Y H 2010 *Chin. Phys. B* **19** 043103
[47] Delley B 1990 *J. Chem. Phys.* **92** 508
[48] Delley B 2000 *J. Chem. Phys.* **113** 7756
[49] Hammer B 1999 *Phys. Rev. B* **59** 7413
[50] Yuan D W, Wang Y and Zeng Z 2005 *J. Chem. Phys.* **122** 114310
[51] Lu J, Wei S H, Zhang Y Y, Hua D Y and Duan X M 2016 *Comput. Theor. Chem.* **1090** 157
[52] Zhao G F and Zeng Z 2006 *J. Chem. Phys.* **125** 014303
[53] Guo J J, Yang J X and Die D 2009 *J. Mol. Struct. ThEOCHEM* **896** 1
[54] Guo J J, Shi J, Yang J X and Die D 2007 *Physica B* **393** 363
[55] Häkkinen H, Yoon B, Landman U, Li X, Zhai H J and Wang L S 2003 *J. Phys. Chem. A* **107** 6168
[56] Lu P, Kuang X Y, Mao A J, Wang Z H and Zhao Y R 2011 *Mol. Phys.* **109** 2057
[57] Guo J J, Yang J X and Xu S L 2008 *J. Atom. Mol. Phys.* **4** 17
[58] Bligaard T, Nørskov J K, Dahl S, Matthiesen J, Christensen C H and Sehested J 2004 *J. Catal.* **224** 206